

# Linear and Nonlinear Soil-Structure Interaction Analysis of Buildings and Safety-Related Nuclear Structures

Chandrakanth Bolisetti<sup>11\*</sup>, Andrew S. Whittaker<sup>22</sup>, Justin L. Coleman<sup>13</sup>

<sup>1</sup>Idaho National Laboratory, 2525 Fremont Avenue, Idaho Falls, Idaho 83402, USA

<sup>2</sup>University at Buffalo, The State University of New York, North Campus, 230 Ketter Hall, Amherst, New York 14260, USA

\*Corresponding author

chandrakanth.bolisetti@inl.gov

awhittak@buffalo.edu

justin.coleman@inl.gov

## Abstract:

Soil-structure interaction (SSI) analysis is generally a required step in the calculation of seismic demands in nuclear structures, and is currently performed using linear methods in the frequency domain. Such methods should result in accurate predictions of response for low-intensity shaking, but their adequacy for extreme shaking that results in highly nonlinear soil, structure or foundation response is unproven. Nonlinear (time-domain) SSI analysis can be employed for these cases, but is rarely performed due to a lack of experience on the part of analysts, engineers and regulators. A nonlinear, time-domain SSI analysis procedure using a commercial finite-element code is described in the paper. It is benchmarked against the frequency-domain code, SASSI, for linear SSI analysis and low intensity earthquake shaking. Nonlinear analysis using the time-domain finite-element code, LS-DYNA, is described and results are compared with those from equivalent-linear analysis in SASSI for high intensity shaking. The equivalent-linear and nonlinear responses are significantly different. For intense

---

<sup>1</sup> Tel.: +1 (208) 526 8161

<sup>2</sup> Tel.+1 (716) 645 4364

<sup>3</sup> Tel. +1 (208) 526 4741

shaking, the nonlinear effects, including gapping, sliding and uplift, are greatest in the immediate vicinity of the soil-structure boundary, and these cannot be captured using equivalent-linear techniques.

## 1. Introduction

Soil-structure-interaction (SSI) analysis is routinely performed on safety-related nuclear structures, including nuclear power plants, in the United States, in support of both design and seismic probabilistic risk assessment. The use of such analysis for the seismic design of buildings is becoming more common but it is not used in mainstream practice because the effects of soil-structure-interaction analysis are assumed to be beneficial, measured here in terms of reduced demands on structural components and floor and wall-mounted equipment.

This paper studies equivalent-linear and nonlinear SSI analysis, with an emphasis on safety-related nuclear structures. Emphasis is placed on nuclear structures because SSI analysis is by-and-large always required by the regulatory authorities to support a design. However, many buildings have construction types and dynamic properties similar to those of nuclear structures, and so conclusions drawn regarding the latter can be directly applied to the former.

The state of practice in SSI analysis in the US nuclear industry involves the use of frequency-domain codes, such as SASSI (Lysmer *et al.*, 1999), with equivalent-linear, strain-compatible properties used to represent the soil. These methods should accurately predict responses for low intensity ground shaking that produces near linear response in the soil. For intense earthquake shaking involving large soil strains and possible gapping and sliding at the foundation-soil interface, nonlinear analysis is theoretically more appropriate because the inelastic effects are captured explicitly. Nonlinear SSI analysis is only possible in the time domain and the numerical tools and codes required to perform these analyses have been developed only recently. Analysts, engineers and regulators will have to gain more experience with nonlinear SSI analysis before the method is broadly accepted for design and risk assessment. A first step is to compare predictions of equivalent linear and nonlinear codes for low intensity shaking, where results should be similar.

A few studies have compared results of frequency-domain and time-domain SSI analysis. Xu *et al.* (2006) compared predictions made using SASSI and LS-DYNA (LSTC, 2013) from SSI analyses of deeply embedded nuclear structures. They observed that results calculated using SASSI and LS-DYNA differed considerably for both linear and nonlinear analyses, with differences in results of linear analyses stemming from differences in the damping formulations. Similar studies by Anderson *et al.* (2013) and Coronado *et al.* (2013) showed that the linear SSI analyses of deeply embedded nuclear structures using time-domain and frequency-domain codes produced very similar structural responses. In these studies, Anderson *et al.* compared results from SAP2000 (Computers and Structures Inc., 2011) to those from SASSI2010 (Ostadian and Deng, 2011), and Coronado *et al.* compared results from the extended subtraction method in SASSI2010 to those calculated using the commercial finite-element code ANSYS (ANSYS Inc., 2013). Spears and Coleman (2014), in a comprehensive study, developed a methodology for performing nonlinear SSI analysis in the time domain, compared the SSI responses calculated using this methodology with those from SASSI, and identified some issues regarding the usage of these codes.

More benchmarking studies are required to support the implementation of nonlinear SSI analyses. These studies should examine cases involving material nonlinearities in the soil and the structure, and geometric nonlinearities, such as gapping and sliding of the foundation, neither of which, can be explicitly simulated in the frequency domain. This paper presents an assessment of the frequency-domain code, SASSI, and the time-domain code, LS-DYNA, for such cases. Analysis using these codes is described in Section 2. A benchmarking study comparing SASSI and LS-DYNA responses of simple, linear structures and soil profiles is presented in Section 3. The benchmarked time-domain analysis procedure is used for nonlinear SSI analyses of two surface-founded structures and the results are compared with those from SASSI. The SASSI analyses are performed using equivalent-linear soil properties and ignoring gapping and sliding at the foundation: the state-of-the-art approach of the US nuclear industry. The results of these analyses and observations regarding the differences between equivalent-linear and nonlinear responses at various ground motion intensities are presented in Section 4.

To maximize the utility of the paper, LS-DYNA keywords are identified where appropriate. This will enable the interested reader to build an understanding of the associated numerical model a) via material that is available at the LSTC website, and b) via reference to Bolisetti and

Whittaker (2015). Such models are not described in detail here. Importantly, reference to LS-DYNA and its keywords is not an endorsement, and a user of another commercial finite element code (e.g., ABAQUS and ANSYS) can map the LS-DYNA keywords to models and algorithms in that code.

## 2. Numerical codes

### 2.1 SASSI

The System for Analysis of Soil-Structure Interaction (SASSI) is the most widely used code for SSI analysis in the nuclear industry. Originally developed by a team at the University of California at Berkeley, several versions of the code are now available. The version distributed by University of California, Berkeley and Ostadan (2010), SASSI2000, is used for the frequency-domain analysis described in this paper.

SASSI uses a sub-structuring method to perform SSI analysis and is capable of two- and three-dimensional analysis of any foundation shape or superstructure (Ostadan, 2006b; Ostadan, 2006a). The sub-structuring method is based on the principle of superposition and is therefore limited to linear analysis. A soil profile in SASSI is composed of infinitely horizontal layers. The soil and structural materials are modeled as linear viscoelastic. Each layer in the soil profile is defined by a layer thickness and a set of material properties; the structure is modeled using finite elements. The sub-structuring method allows the soil-structure model to be solved in parts: 1) calculation of free-field soil response (site-response analysis), 2) calculation of impedance functions at the foundation (impedance analysis), and 3) calculation of structural response (structural analysis). Equivalent-linear, strain compatible properties are used for the soil, which are calculated for each ground motion input using an equivalent-linear site-response code such as SHAKE2000 (Schnabel *et al.* 2009).

### 2.2 LS-DYNA

LS-DYNA is a commercial finite-element code capable of three-dimensional nonlinear analyses. It is equipped with a large number of material models that can be used for soil and structure and several contact models suitable for a soil-foundation interface. LS-DYNA has been used for nonlinear site-response and SSI analyses of buildings and petrochemical structures

(Willford *et al.*, 2010). Soil-structure interaction analysis in LS-DYNA can be performed using either the direct method or the Domain Reduction Method<sup>4</sup> [DRM; Bielak *et al.*, (2003)].

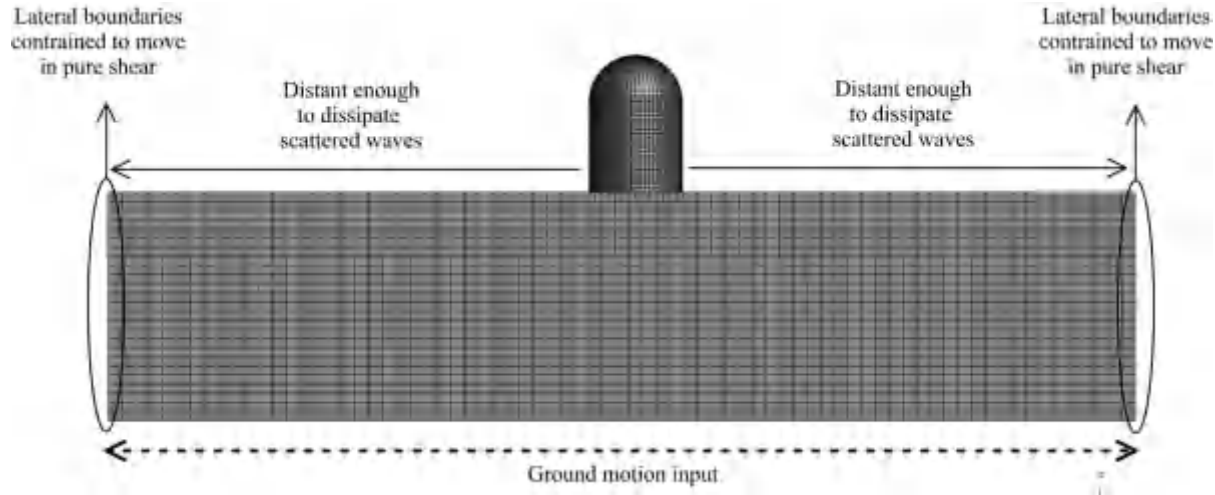
The direct method involves analysis of the entire soil-structure system in a single step, thus circumventing the use of superposition, which is restricted to linear analyses. This enables simulation using nonlinear material models for the soil and structure, and contact models that allow separation and sliding at the soil-foundation interface. Soil-structure interaction analysis using the direct method can also be performed using other commercial finite-element codes such as ABAQUS (Dassault Systèmes, 2005), ANSYS, or the open source codes, OpenSees (Mazzoni *et al.*, 2009) and MOOSE (Gaston *et al.*, 2009).

Figure 1 describes a finite-element model for SSI analysis using the direct method. In this method, an infinite soil domain is simulated by a finite soil domain that 1) effectively damps the scattered waves radiating away from the structure, and 2) provides free-field stress equilibrium at the lateral boundaries. The former can be achieved using absorbing boundaries such as the viscous boundary model by Lysmer and Kuhlemeyer (1969) and the Perfectly Matched Layer (PML) model (Basu, 2009), both of which, have been implemented in LS-DYNA, and infinite element implemented in ABAQUS. However, these boundary models are 1) limited to linear materials and 2) do not simulate the free-field stress condition required at the lateral boundaries. No absorbing boundary models have yet been developed for nonlinear materials to the knowledge of the authors. A reasonable approach to simulating an infinite domain at this time is to build a large soil domain with sufficient plan dimensions to dissipate the radiating waves, and constraining the lateral boundaries to move in pure shear, thus simulating a free-field condition. In this approach, the radiating waves dissipate through soil hysteresis and viscous damping in the soil. The pure shear constraint is achieved by forcing nodes at the same elevation to move together in the horizontal and vertical directions, assuming that the input ground motion consists of vertically propagating waves. The input ground motion is imposed at the base of the soil domain as either 1) a stress input (if outcrop motion is available), or 2) acceleration input at depth (if within profile motion is available). The method of imposing the within or outcrop ground motion is identical to that in a one-dimensional site-response analysis. This method is

---

<sup>4</sup> This method is referred to as the Effective Seismic Input method in the LS-DYNA keyword manual (LSTC, 2013). The Effective Seismic Input method, proposed by Bielak and Christiano (1984), is a predecessor to the DRM, but is practically equivalent (Bielak, 2013).

described in Bolisetti and Whittaker (2015) and Kwok *et al.*, (2008). Coleman *et al.*, (2015) presents a detailed description of the direct method and identifies issues that must be addressed when using it to perform nonlinear SSI analysis.



**Figure 1:** Finite-element model for soil-structure interaction analysis using the direct method  
(Bolisetti and Whittaker, 2015)

The DRM enables the input of complex, three-dimensional wave-fields for site-response and SSI analysis within a finite-element framework and it is available in LS-DYNA (Basu, 2011). Linear SSI analysis using the DRM was performed in LS-DYNA and results can be found in Bolisetti and Whittaker (2015). The DRM has been successfully used for large-scale SSI simulations in computational seismology (Day *et al.*, 2006; Taborda, 2010; Taborda and Bielak, 2011; Xu, 1998; Xu *et al.*, 2003; Yoshimura *et al.*, 2003) and can be used for site-response and SSI analyses such as those presented in this paper. However, because the scope of this study is limited to vertically propagating shear waves, the direct method is used here.

### 3. Benchmarking LS-DYNA using SASSI for linear analysis

Benchmarking is a code-to-code verification. SASSI results are used here to benchmark LS-DYNA using simple structures founded near the surface of a uniform soil profile. The profile is 29.5m deep and the soil is a linear viscoelastic with a mass density of  $1700 \text{ kg/m}^3$ , shear wave velocity of 165 m/s, Poisson's ratio of 0.3, and a damping ratio of 0.02. Two lumped-mass structures are considered: 1) a 10m tall structure (LM1) with a lumped mass at its tip, and 2) a 25.6m tall structure (LM2) with lumped masses at the tip, mid-height and base. These structures

have fixed-base natural periods of 0.23 sec and 0.14 sec, respectively. Both are founded on a basemat with plan dimensions of 13.8m × 3.8m and a thickness of 1.4m, which is embedded a distance equal to its thickness. Model LM1 is designed to produce minimal SSI effects whereas LM2 responds predominantly in a rocking mode with significant SSI effects. More information on the structures (masses, beam cross-section properties) is provided in Bolisetti and Whittaker (2015).

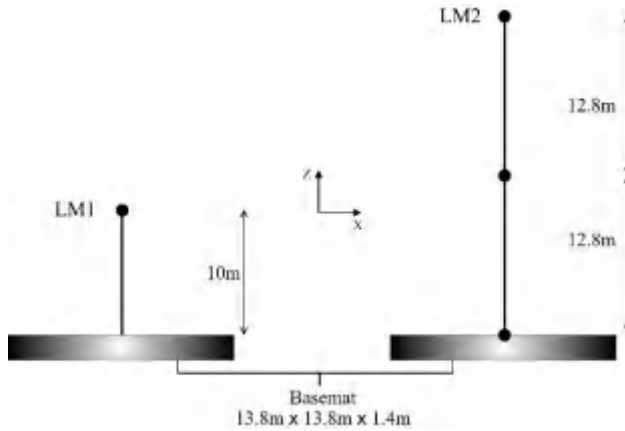


**Figure 2:** Lumped-mass structures, LM1 and LM2, used for linear SSI analysis

These superstructures are modeled in both SASSI and LS-DYNA using beam elements and lumped masses; the basemat is modeled using eight-noded brick elements. The SASSI soil domain comprises infinitely horizontal layers, and the thickness of these layers is determined by the minimum wavelength (maximum frequency) that needs to be propagated through the soil profile in the analysis. For a given maximum frequency, the maximum layer thickness is calculated from the equation

$$t_{\max} \leq \frac{\lambda_{\min}}{n} = \frac{V_s}{n \cdot f_{\max}} \quad (1)$$

where  $t_{\max}$  is the maximum thickness of the soil layers,  $\lambda_{\min}$  is the minimum wavelength of the shear waves,  $V_s$  is the shear wave velocity,  $f_{\max}$  is the maximum frequency of the shear waves, and  $n$  is the desired number of layers per shortest wave length. The inequality in this equation governs the ‘resolution’ with which the shortest wavelength is captured during wave propagation through the soil layers. For example, when a value of 10 is used for  $n$ , the shortest wavelength

is captured by at least 10 soil layers, namely 10 values of displacement. A larger value of  $n$  results in a higher resolution of the wave propagation in the soil profile but at greater computational requirements. The SASSI manual recommends a minimum value of 5 for  $n$ . A value of 10 is used in the analyses of this study. The SASSI soil profile is therefore discretized into 29 layers to allow a maximum frequency of 15Hz, which is deemed sufficient for the SSI analysis presented here. The SASSI user manual (Ostadian, 2006) recommends performing analysis (calculating the transfer functions) at 10 to 20 frequencies but analysis at 20 frequencies was found to be insufficient (Bolisetti and Whittaker, 2015) and 44 frequencies ranging from 0.02Hz to 25Hz are used instead

The LS-DYNA soil domain is 218m  $\times$  118m (218m in the shaking direction, X) in plan, 29.47m deep, and is built using eight-node solid elements (Figure 3). The adequacy of the soil domain size is verified by comparing the horizontal surface response at its boundaries to the corresponding surface free-field response calculated using one-dimensional site-response analysis performed separately in LS-DYNA. Section 3.1.1 presents the results of these analyses and demonstrates that the soil-domain is large enough to dissipate the outgoing waves scattered from the structure. The element size in the soil domain is limited to 1m, which allows the propagation of frequencies up to 15Hz at 10 elements per wavelength, for the shear wave velocity of 165 m/s (see Equation 1).

The superstructure and basemat are connected using rigid beams. SASSI does not have a rigid material model (unlike LS-DYNA) and so these beams are modeled using either a very large elastic modulus or large cross-section properties. A frequency-independent damping ratio of 0.02 is used for the soil and the structure in both SASSI and LS-DYNA. While a frequency-independent damping ratio is simulated in SASSI by default, it is (approximately) achieved in LS-DYNA using the \*DAMPING\_FREQUENCY\_RANGE option. The basemat-soil interface in LS-DYNA is modeled with a tied contact that does not allow separation.



**Figure 3:** LS-DYNA finite element model for SSI analysis of LM2 using the direct method

Eigen value analysis of the structural models with a fixed base is performed in SASSI and LS-DYNA to confirm that their dynamic properties are identical. The models LM1 and LM2 are analyzed for three cases: 1) rigid superstructure on a rigid basemat, and 2) flexible superstructure on a rigid basemat, and 3) flexible superstructure on a flexible basemat. The SASSI and LS-DYNA results for each case are compared in Section 3.1. The comparisons are made for a single input motion: an Ormsby wavelet (Ryan, 1994). The Ormsby wavelet features a Fourier transform with a constant amplitude in a specified frequency range. This wavelet therefore provides a convenient alternative to real earthquake ground motions, which typically have considerable contribution from (and therefore biased to) a relatively narrow spectrum of frequencies. The Ormsby wavelet used for the benchmarking study has a peak acceleration of 0.5g and constant Fourier transform amplitude between 0.2 and 20Hz. The wavelet is applied at the base of the soil domain as an acceleration input, assuming that the soil profile is underlain by a rigid bedrock.

### **3.1 Analysis results and comparisons between SASSI and LS-DYNA**

#### **3.1.1 Free-field response**

Figure 4 presents the free-field response of the soil domain to an Ormsby wavelet calculated using SASSI and LS-DYNA SSI analyses, and a separate one-dimensional site-response analysis (SRA) performed in LS-DYNA. The free-field response in the LS-DYNA SSI model is taken as

the response of the soil at surface in the corner of the domain shown in Figure 3. The response of the same point in the SASSI model is considered to be the SASSI free-field response. The one-dimensional SRA in LS-DYNA is performed using a single stack of solid elements, with each element corresponding to a layer of solid elements in the SSI model shown in Figure 3. A detailed description of one-dimensional SRA in LS-DYNA is provided in Bolisetti *et al.* (2014) and Bolisetti and Whittaker (2015), and is not reproduced here.

Panel a of Figure 4 presents 1% damped response spectra, and the panel b presents the Fourier transforms of the acceleration at the surface of the soil domain. The free-field responses calculated using the two codes are almost identical. The small differences in the peak amplitudes are attributed to the different damping formulations in the two codes. A notable feature of these results is the peaks in the response spectra and the Fourier transforms. These peaks correspond to the natural frequencies of the soil profile, which can be calculated using the expression,  $(2n-1)V_s/4H$ , where  $n$  is the vibration mode number,  $V_s$  is the shear wave velocity of the material, and  $H$  is the total depth of the soil profile (Kramer, 1996). The peaks in the Fourier transforms presented in Figure 4 show that the vibration modes occur at 1.4Hz, 4.2Hz, 7Hz, 9.8Hz, and so on. These frequencies are identical to those calculated using the above expression.

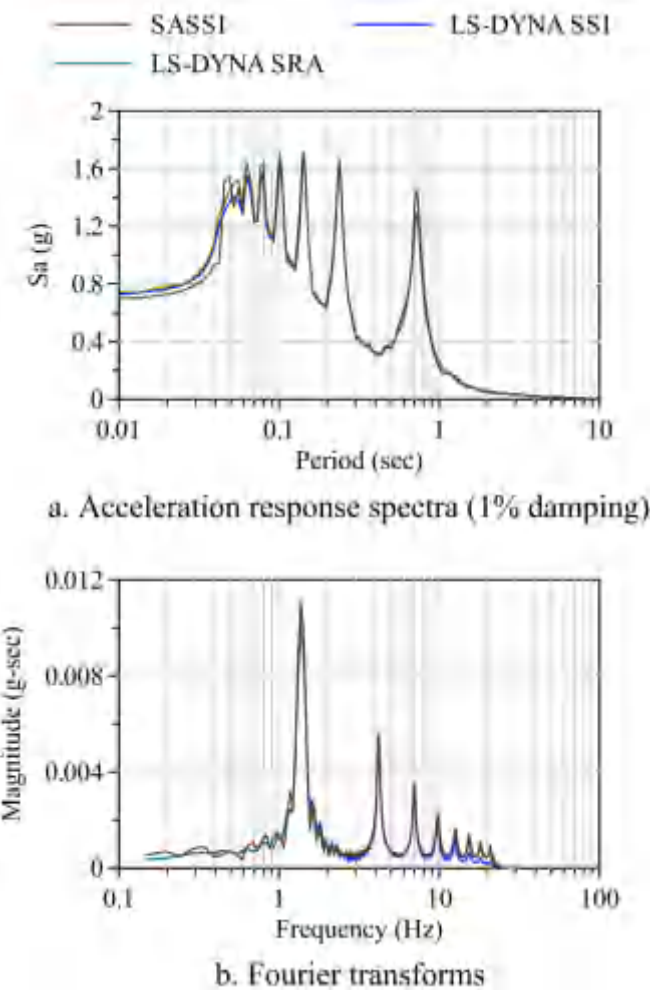


**Figure 4:** Surface free-field accelerations computed using site-response analysis and the SSI analysis for LM2

### 3.1.2 Fixed-base response

Figure 5 presents the 1% damping response spectra of the horizontal accelerations at the roof of the fixed-base models of LM1 and LM2 calculated using SASSI and LS-DYNA. These response spectra are almost identical, indicating that the fixed-base models of the structures in SASSI and LS-DYNA are equivalent, with the small differences again attributed to the damping formulations. Structures LM1 and LM2 have fixed-base natural periods of 0.23 sec and 0.14 sec, respectively.

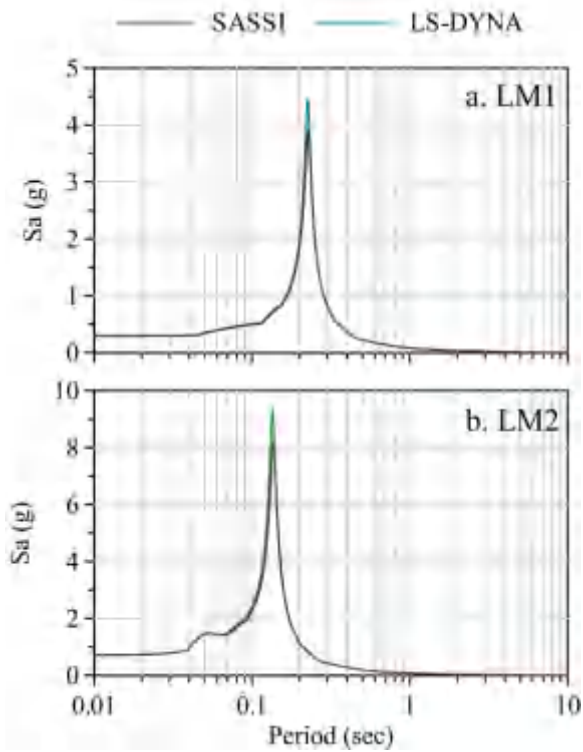


**Figure 5:** Response spectra (1% damping) of the roof accelerations of the fixed-base models calculated using SASSI and LS-DYNA

### 3.1.3 SSI response of LM1

Figure 6 presents the amplification of the 1% damped horizontal acceleration spectrum at the roof of structure LM1 from the free-field surface of the soil for three cases: rigid structure on a rigid basemat, flexible structure on a rigid basemat, and flexible structure on a flexible basemat. For each case, the amplification is calculated using SASSI and LS-DYNA. The figure shows that the amplification calculated using the two codes are almost identical for all cases. A comparison of the responses in the second and third panels of the figure indicates that the flexibility of the basemat decreases the peak structural amplification for LM1. Figure 6 also shows that the flexible-base period of LM1 is about 0.6 sec, which is about 2.5 times the fixed-base period of 0.23 sec, indicating significant period lengthening due to SSI effects.

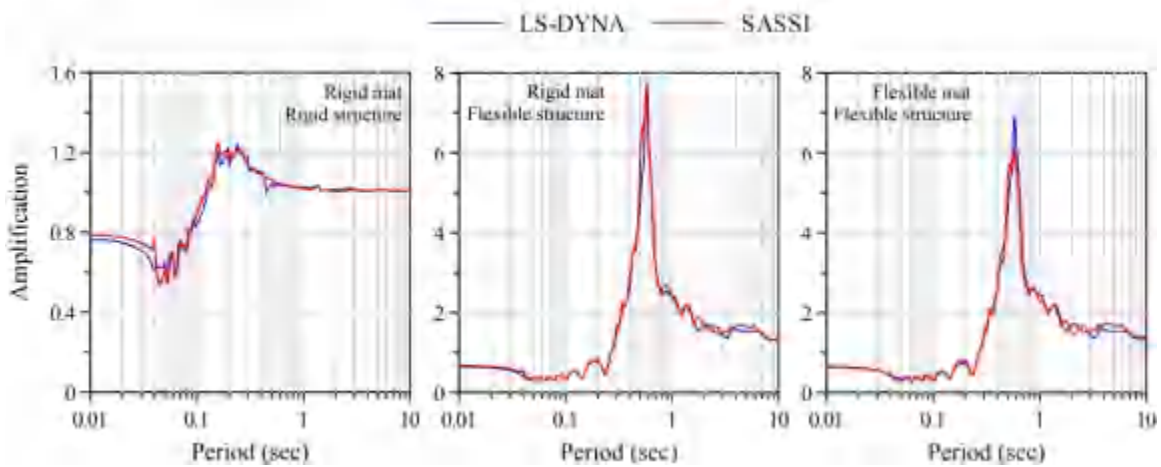


**Figure 6:** Acceleration amplification spectra (1% damping) from the surface free field of the soil to the roof of LM1

### 3.1.4 SSI response of LM2

Similar to Figure 6, Figure 7 presents the amplification of the 1% damped horizontal acceleration spectrum at the roof of LM2 calculated using SASSI and LS-DYNA for the three analysis cases. The first panel of the figure shows that spectral amplifications are almost identical for the analysis case with a rigid structure on a rigid basemat. However the second and third panels show that the peak amplifications calculated using SASSI are slightly greater than those calculated using LS-DYNA. These differences are greater than those seen for LM1. Again, this can be attributed to the damping formulations of the two codes, and specifically to the fact that the damping ratio in LS-DYNA is only approximately frequency-independent. In contrast with LM1, accounting for basemat flexibility slightly increases the peak structural amplifications of LM2, indicating that the impact of basemat flexibility on structural response depends on the flexible-base period of the structure. Figure 7 also shows that the flexible-base period of LM2 is about 0.42 sec, which is about three times the fixed-base period of 0.14 sec indicating significant period lengthening due to SSI effects.

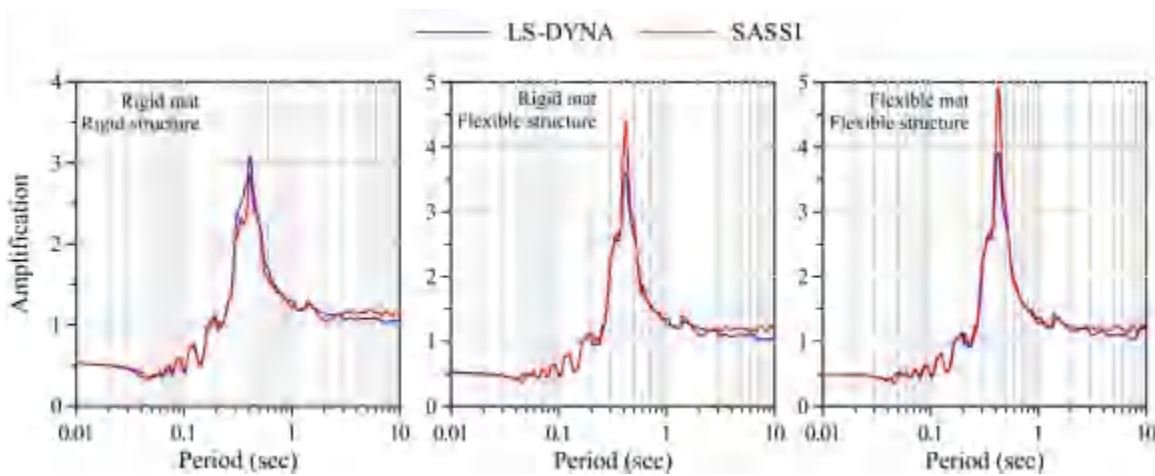


**Figure 7:** Acceleration amplification spectra (1% damping) from the surface free field of the soil to the roof of LM2

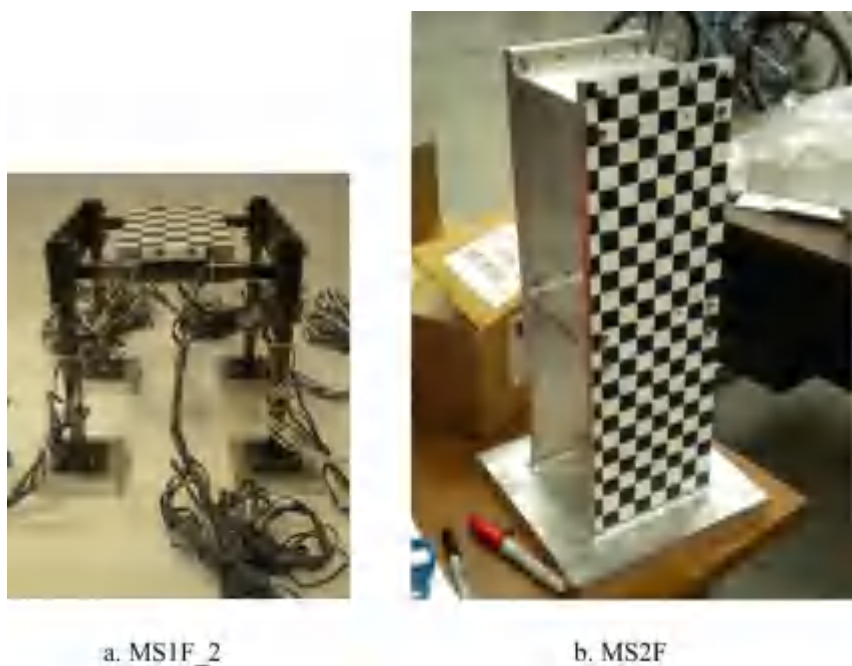
#### 4. Assessment for nonlinear SSI analysis

After verifying that the direct method of SSI analysis in LS-DYNA produces almost identical results as SASSI for linear elastic analysis, this procedure is used to perform nonlinear SSI analyses, and the results are compared to equivalent-linear analyses in SASSI. The nonlinear SSI analyses are performed for two structures subjected to four ground motions with different intensities and frequency characteristics. The soil profile, structural models and input ground motions used for nonlinear analyses are those from the NEES City Block project (Mason *et al.*, 2010a; Mason *et al.*, 2010b; Mason *et al.*, 2011), which involved the investigation of structure-soil-structure interaction (SSSI) in dense urban regions through centrifuge tests and numerical simulations involving several building models. However, the numerical responses of these building models are not compared with the experimental data from the City Block project because an appropriate simulation of the centrifuge experiments requires consideration of several factors, such as boundary effects from the laminar box and interaction of the shaker with the centrifuge bucket, neither of which were addressed in the project. A qualitative comparison of the numerical and experimental results can be found in Bolisetti and Whittaker (2015).

##### 4.1 Structural models and soil profile

The City Block tests used dense, dry Nevada sand at a relative density of 80%. The soil in the laminar box was 29.5m deep at the prototype scale and had a unit weight of 16.66 kN/m<sup>3</sup>. Two

building models are adopted from the City Block project for the nonlinear SSI analyses of this section: 1) a one-story, steel moment-resisting frame founded on footings (hereafter referred to as MS1F\_2), and 2) a two-story shear wall building founded on a basemat (hereafter referred to as MS2F). These building models had realistic superstructure and foundation designs, and using these models for numerical analysis provides insight into nonlinear SSI effects in buildings commonly encountered in practice. Additionally, a highly nonlinear foundation response is anticipated, which makes these models appropriate for the comparison of frequency-domain and time-domain codes. The two structures MS1F\_2 and MS2F had 1<sup>st</sup> mode fixed-base natural periods of 0.13 sec and 0.47 sec, respectively, at the prototype scale. Additionally, the building models were designed to have a flexible-base natural period close to 0.6 sec, which is equal to the first mode natural period of the soil profile. This was expected to amplify the SSI effects in the building models. Preliminary numerical analyses by Mason *et al.* (2011) showed that MS1F\_2 and MS2F had the 1<sup>st</sup> mode flexible-base natural periods 0.65 sec and 0.60 sec, respectively, at the prototype scale. The experimental model of MS1F\_2 was designed to exhibit nonlinear behavior through the formation of plastic hinges in the beams and columns, but the shear wall structure, MS2F, was designed to remain elastic for all ground motions. Nonlinearity in MS1F\_2 was achieved by reducing the cross-sectional areas of the beams and columns over a certain length at the locations where plastic hinges were expected. These potential plastic hinges or ‘fuses’ were provided close to the beam-column joints and at the base of the columns. A detailed description of the designs of MS1F\_2 and MS2F and their experimental models are presented in Mason *et al.* (2011), Mason (2011), Trombetta (2013) and Bolisetti and Whittaker (2015). The corresponding numerical models in SASSI and LS-DYNA are described in Sections 4.3 and 4.4, respectively. Photographs of the building models used in the experiments are presented in Figure 8.



a. MS1F\_2

b. MS2F

**Figure 8:** Photographs of the building models used in the City Block project

#### 4.2 Input ground motions

The ground motions used for this study are also those from the City Block project. The City Block project used a suite of nine ground motion recordings from six earthquakes, which are representative of the seismicity of downtown Los Angeles. These ground motions included ordinary and near-fault, pulse-like motions with forward directivity (Somerville *et al.* 1997). A more detailed description of the selection and scaling process of these ground motions is presented in Mason *et al.* (2010). Four of these ground motions are used here for the nonlinear SSI analyses. Details of ground motions are provided in Table 1. The 5% damped acceleration response spectra of the ground motions are presented in Figure 9. These ground motions are input at the base of the soil profile as ‘within’ motions.

**Table 1:** Input ground motions used for nonlinear SSI analyses

GM #	Ground Motion ID	Earthquake	Station	Type <sup>a</sup>	Peak <sup>b</sup>
5	JOS_L	92 Landers	Joshua Tree 090	Ord	0.06
10	LCN	92 Landers	Lucerne 260	NF, FD	0.26
12	SCS_H	94 Northridge	Sylmar Conv Sta. 052	NF, FD	0.58
13	PRI_H	95 Kobe	Port Island-Mod-79m	NF, FD	0.64

<sup>a</sup> Type of ground motion: Ord stands for ordinary, NF stands for near fault and FD stands for forward directivity

<sup>b</sup> Input peak acceleration (at the base of the soil profile)

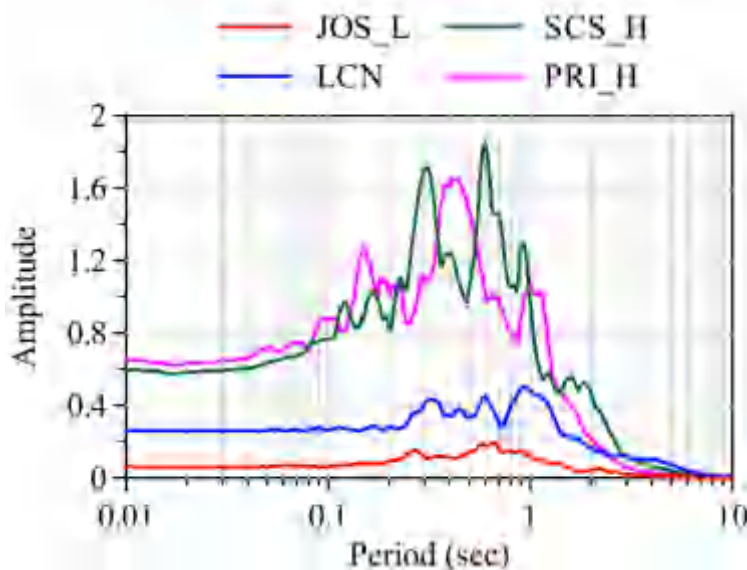


**Figure 9:** Acceleration response spectra (5% damping) of the input ground motions

### 4.3 Modeling in SASSI

Since SASSI performs a linear elastic analysis, nonlinear SSI response is approximated by using strain-compatible properties (shear modulus and damping ratio) for each soil layer. These properties depend on the peak shear strain imposed by the input ground motion, and are calculated using the equivalent-linear site-response analysis code SHAKE2000 which, apart from the site response, outputs the strain-compatible shear moduli and damping ratios of the soil

layers. The SASSI soil profile for nonlinear SSI analysis is therefore different for each input ground motion.

Prior to modeling the soil profile for nonlinear analysis, one-dimensional site-response analysis is performed using SHAKE for each of the four ground motions to calculate the strain-compatible soil properties. The small-strain shear wave velocities presented in Figure 10 are used as an input for these SHAKE analyses. Site-response analysis using SHAKE also requires modulus reduction and damping curves, which describe the decrease in shear modulus and increase in damping ratio with an increase in the shear strain in the soil [see Bolisetti *et al.* (2014)] for a description of equivalent-linear material models]. The modulus reduction and damping curves developed by Seed and Idriss (1970) for sands are used for the analyses in this study. The lower bound modulus reduction curve and the upper bound damping curve, both of which are available in the SHAKE database, are employed in the site-response analyses. As seen in the figure, the soil profile is discretized into 29 layers. The strain-compatible properties, calculated using SHAKE, are also presented in Figure 10 for each of the four ground motions. This discretization of the soil profile allows a maximum frequency of 9Hz (using  $n=10$  in Equation 1), which is adequate for the analyses presented in this section. A more detailed description of the site-response analyses in SHAKE is presented in Bolisetti and Whittaker (2015). Poisson's ratio of 0.3 (Kulhawy and Mayne, 1990) and a unit weight of 16.66 kN/m<sup>3</sup> are used for all the soil layers.

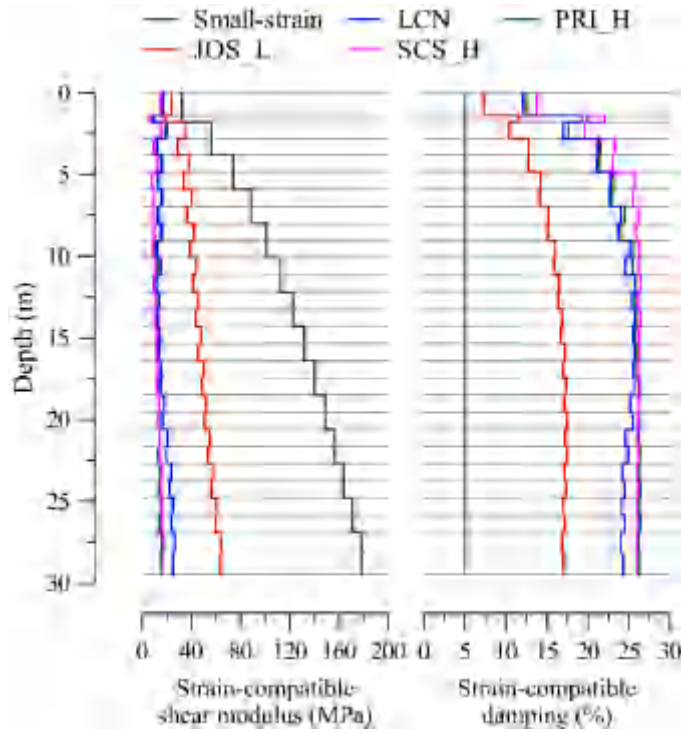


**Figure 10:** Small-strain and strain-compatible shear moduli and damping ratios used for SSI analyses using SASSI for simulation of Tests 3 and 4

The ground motions listed in Table 1 are input to the SASSI models at the base of the soil profile assuming rigid bedrock. The superstructures are modeled using beam elements with lumped masses at the nodes. Each beam and column of MS1F\_2 is modeled using a beam element, and the roof mass is lumped at the nodes. The shear walls at each floor of MS2F are combined and modeled as a single beam element, resulting in a lumped-mass ‘stick’ model. The beam cross-section properties and roof masses used for both structures are first calculated from the experimental models, and then calibrated through a fixed-base analysis to match the fixed-base natural periods calculated through hammer tests performed before the experiments. Nonlinear behavior in the superstructure of MS1F\_2 is not modeled in SASSI. The foundations (footings of MS1F\_2 and basemat of MS2F), and the corresponding excavated soil, are modeled using solid elements, and are embedded to a depth equal to their thickness. The column-foundation connections of both buildings are modeled using stiff beam elements as shown in Figure 11. Further specifications of the numerical models of the superstructure (beam cross-section properties, roof masses, etc.) can be found in Bolisetti and Whittaker (2015). The SASSI numerical models of MS1F\_2 and MS2F are presented in Figure 11.

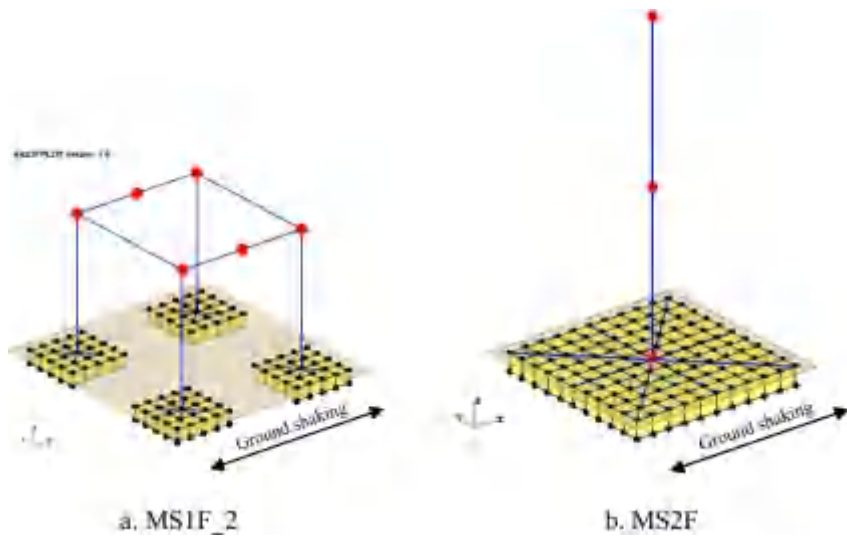


**Figure 11:** Numerical models MS1F\_2 and MS2F for SASSI analysis

#### 4.4 Modeling in LS-DYNA

Nonlinear SSI analyses in LS-DYNA are performed using the direct method. The soil domain of the LS-DYNA model is 219m × 118m in plan (219m in the shaking direction, X) and 29.5m deep (equal to the depth of the soil profile in the City Block project at prototype scale), and is built using eight-node solid elements. The largest plan dimension is about 16 times the size of the basemat of MS2F and 15 times the plan dimension of MS1F\_2. The input ground motion is applied as acceleration input at the base, which is consistent with the assumption of rigid bedrock. The LS-DYNA model for the nonlinear analysis of MS2F is presented in Figure 12.

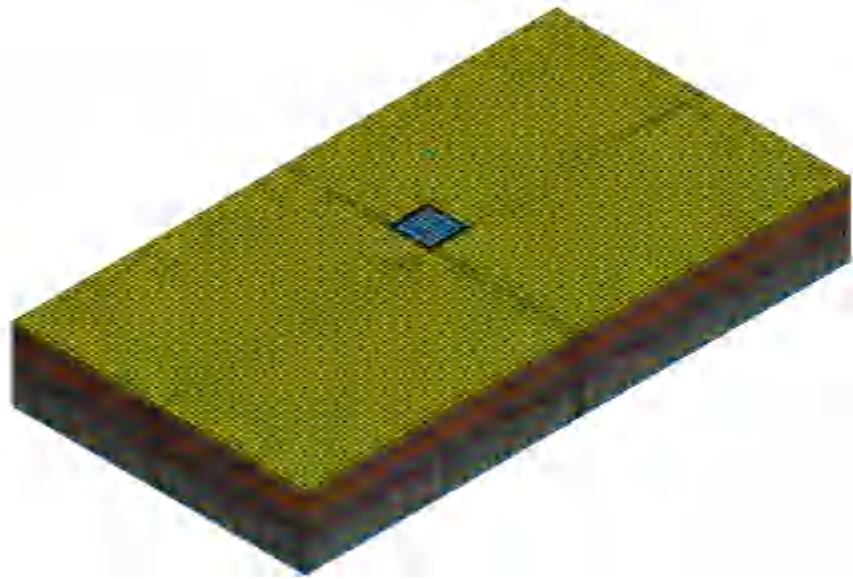


**Figure 12:** LS-DYNA finite element model for SSI analysis of MS2F

The soil material in LS-DYNA is modeled using the \*MAT\_HYSTERETIC\_SOIL model (LSTC, 2013), which is capable of simulating three-dimensional nonlinear, hysteretic constitutive behavior. The hysteretic behavior of this material model follows a piece-wise linear backbone curve, which is input by the user as ten pairs of shear stress and shear strain values. This backbone curve is internally transformed into ten elastic-perfectly-plastic ‘layers’ that respond in parallel, similar to the distributed element modeling concept developed by Iwan (1967). Each of these elastic-perfectly-plastic layers is defined by an elastic modulus and a yield stress, and follows Von-Mises failure criterion at yield, similar to the distributed-element models developed by Chiang and Beck (1994) for the simulation of cyclic plasticity. The shear stress and shear strain values for input in LS-DYNA are calculated from the modulus reduction curves and the low-strain shear moduli used as input in the SHAKE analysis. These calculations are made using the equation

$$\tau(\gamma) = \frac{G}{G_{\max}}(\gamma) \cdot G_{\max} \cdot \gamma \quad (2)$$

where  $\gamma$  is the shear strain in the soil layer,  $\tau(\gamma)$  is the shear stress,  $G_{\max}$  is the small-strain shear modulus of the soil layer (Figure 10) and  $G/G_{\max}(\gamma)$  is the modulus reduction ratio. Similar to the SHAKE and SASSI analyses, the soil domain in LS-DYNA analyses is

constructed using 29 layers, with each layer in SHAKE and SASSI corresponding to a layer of solid elements in LS-DYNA. Soil damping in nonlinear SSI analysis is primarily simulated through nonlinear hysteresis. A small amount of viscous damping is applied to account for damping at very small strains, for which, hysteresis is negligible. A damping ratio of 0.4%<sup>5</sup> is used in the nonlinear analyses of this section using the \*DAMPING\_FREQUENCY\_RANGE\_DEFORM option.

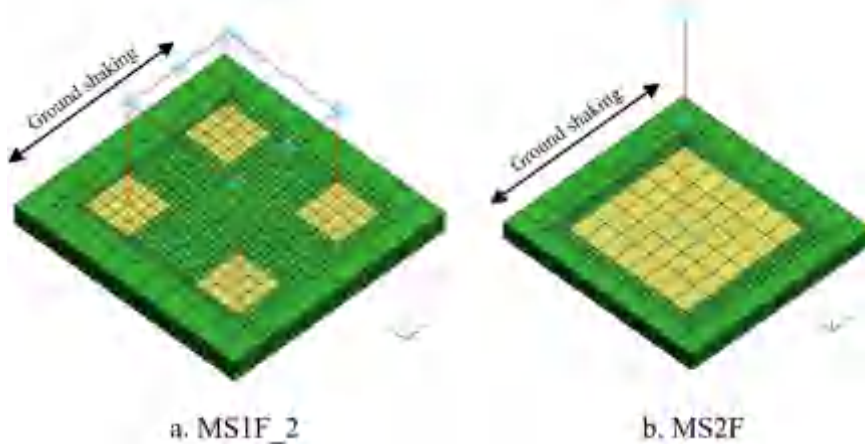
The building models, MS1F\_2 and MS2F, are identically modeled in SASSI and LS-DYNA with beam elements and lumped masses, except that the nonlinear behavior is modeled in LS-DYNA. Nonlinearity in the beams is modeled using the \*MAT\_SEISMIC\_BEAM, available in the LS-DYNA material database (LSTC, 2013). This material model simulates nonlinear behavior at one of the nodes of the beam element in the form of a plastic hinge, which follows a plastic moment-rotation curve input by the user. This plastic moment-rotation curve for the plastic hinges of MS1F\_2 is calculated from a separate pseudo-static analysis of a beam fuse modeled using shell elements in LS-DYNA [refer to Bolisetti and Whittaker (2015) for details]. Two percent damping is provided for the superstructures for frequencies between 1 and 25Hz using the \*DAMPING\_FREQUENCY\_RANGE\_DEFORM option. The footings of MS1F\_2 and the basemat of MS2F are modeled as rigid using solid elements. Both foundations are embedded such that the top of the foundation is at grade.

Figure 13 presents the superstructures, foundations, and soil elements close to the foundations of the SSI models of MS1F\_2 and MS2F. The rest of the soil domain is shown in Figure 12 and is not shown in these figures for clarity. The figure also shows that a finer mesh is used for the soil close to the foundations than in the remainder of the soil domain: to accommodate the large soil strains expected near the foundations. The foundation-soil interface for both the footings and the basemat can modeled as either 1) a ‘tied’ interface with no loss of contact between the soil and the foundation, or 2) a more realistic interface that allows for loss of contact between the soil and the foundation, resulting in sliding, gapping and uplift. The latter contact interface is modeled using the automatic surface-to-surface contact model in LS-DYNA (LSTC, 2013) that employs a penalty-type contact formulation and simulates Coulomb friction in sliding. A friction coefficient of 0.84 is used for the analyses of this study. This friction

---

<sup>5</sup> A 0.4% damping is chosen to be consistent with a separate DEEPSOIL (Hashash *et al.*, 2011) analysis performed as a part of a different, but related, study. Refer to Bolisetti and Whittaker (2015) for details.

coefficient is calculated as  $\tan \phi$ , where  $\phi$  is the friction angle of Nevada sand (used in the City Block experiments), which is estimated to be between 37 and 42 degrees (Mason *et al.* 2011). A friction angle of 40 degrees is used for the analyses presented in this study.



**Figure 13:** Isometric views of the SSI models in LS-DYNA (soil domain not shown for clarity)

#### 4.5 Analysis results and comparison

Nonlinear behavior in a soil-structure system can be classified into 1) nonlinear site response (primary nonlinearities), which affects the free-field soil response, and therefore the ground motion input to the structure and 2) nonlinear behavior at the foundation (soil hysteresis, gapping, sliding) and nonlinear structural behavior (secondary nonlinearities). While SASSI approximately accounts for the primary nonlinearities, LS-DYNA directly accounts for both primary and secondary nonlinearities. Therefore, it is expected that the SSI responses from SASSI and LS-DYNA will be increasingly different as the intensity of the input ground motion is increased and the response of the system is more nonlinear.

The differences in the total acceleration at the roof of a structure calculated using SASSI and LS-DYNA reflect both the primary and secondary nonlinearities in the soil-structure system. Primary nonlinearities are investigated in this study by comparing the surface free-field responses calculated using SASSI and LS-DYNA. Secondary nonlinearities are investigated by examining the roof accelerations relative to the base of the structure, which do not include the free-field acceleration. The roof acceleration of MS1F\_2 is calculated in terms of 1) acceleration relative to the base (one of the footings), and 2) total acceleration. Similarly, since MS2F predominantly responds in the rocking mode, the roof acceleration of this structure is calculated

in terms of 1) acceleration due to rocking, and 2) total acceleration. The former component in the roof acceleration in both the structures is assumed to be primarily influenced by secondary nonlinearities. The use of contact elements in LS-DYNA introduces an artificial high-frequency noise in the acceleration response. Therefore all the LS-DYNA acceleration responses are filtered using a low-pass filter with a cut-off frequency of 10Hz. Since the anticipated flexible-base frequencies of the structures, and the fundamental frequency of the soil profile (all around 1.7Hz) are much smaller than 10Hz, this cut-off frequency is deemed appropriate for the analyses presented in this section. The following sections present the results of these analyses.

#### 4.5.1 Free-field responses

The surface free-field responses of the soil profile are expressed as the 5% damped acceleration response spectra at one of the corners of the soil domain (farthest from the structure) in the LS-DYNA model, and at the same point on the soil surface in the SASSI model. These responses are presented in Figure 14. The figure shows that the SASSI and LS-DYNA predictions of the free-field response are similar for the JOS\_L ground motion and are considerably different for the other ground motions. The LS-DYNA responses are also consistently lower than the corresponding SASSI responses, especially around the periods corresponding to the peak spectral accelerations. This difference is attributed to calculation procedures: the averaging of nonlinear response over time in the equivalent-linear (SASSI) analysis and the explicit simulation of the hysteretic behavior of the soil in LS-DYNA through time. A more detailed comparison of the equivalent-linear and nonlinear site-response analysis codes is presented in Bolisetti *et al.* (2014) and Bolisetti and Whittaker (2015).

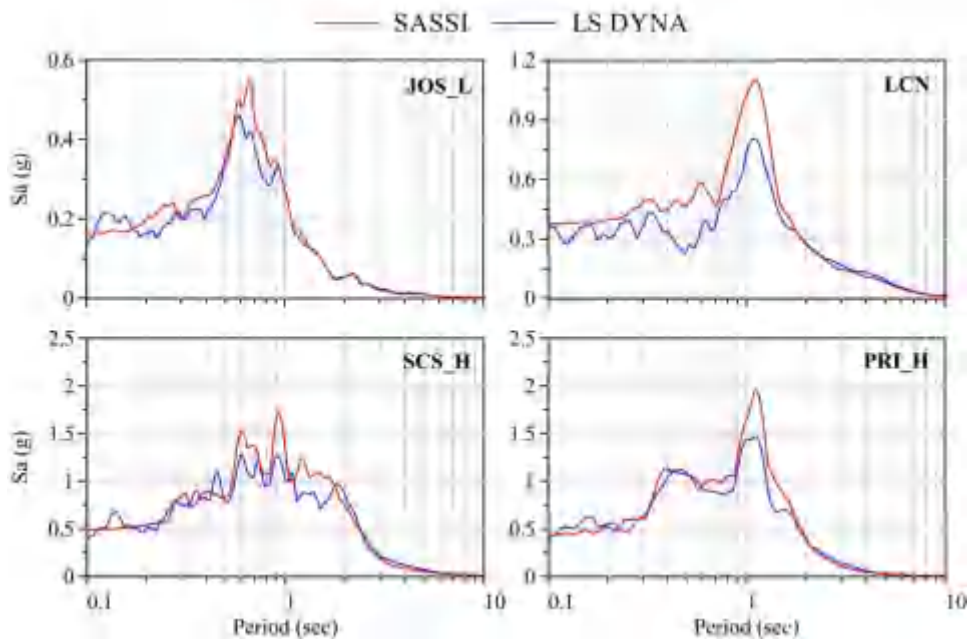


**Figure 14:** Free-field acceleration response spectra (5% damping) at the surface of the soil profile

#### 4.5.2 MS1F\_2

Before comparing the equivalent-linear response in SASSI and the nonlinear response in LS-DYNA, a linear elastic analysis is performed using strain-compatible moduli and 2% damping ratio in both the codes, for the JOS\_L ground motion. Figure 15 presents the 5% damped response spectra of the accelerations relative to the base, and the total accelerations at the roof of MS1F\_2 for this linear elastic analysis. The figure shows that the results are almost identical, demonstrating the equivalence of the SASSI and LS-DYNA SSI models of MS1F\_2 in the linear domain.

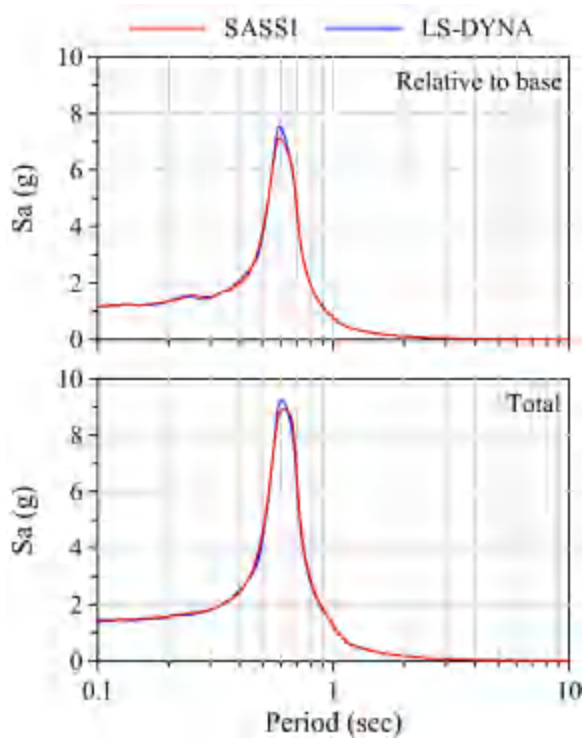


**Figure 15:** Acceleration response spectra (5% damping) at the roof of MS1F\_2 subjected to the JOS\_L ground motion for the preliminary linear analysis

The verified linear models are then modified: equivalent-linear soil properties are included in SASSI, and the nonlinear soil properties and contact interface models are included in LS-DYNA. Analysis results for the four input ground motions, JOS\_L, LCN, SCS\_H and PRI\_H, are presented in Figure 16. In this figure, ‘LS-DYNA (tied)’ and ‘LS-DYNA (separation allowed)’ correspond to the two foundation-soil interface conditions mentioned previously. Contrary to the results of the linear analysis in Figure 15, this figure shows significant differences in the SASSI and LS-DYNA results for both relative and total acceleration responses, even for the JOS\_L ground motion, which has an input acceleration of 0.06g at the base of the soil profile. The peaks in the relative acceleration spectra calculated using LS-DYNA (separation allowed) occur at longer periods than those calculated using SASSI, indicating that the differences arise from increased flexibility either at the foundation or in the superstructure, due to nonlinear behavior. Since the fuses of MS1F\_2 did not yield for this ground motion, the differences in the structural responses are attributed to nonlinear behavior in the soil near the footings. This hypothesis is confirmed by performing a separate nonlinear analysis in LS-DYNA, with the soil at the vicinity

of the footings modeled with linear elastic material, and with a tied foundation condition. Figure 17 presents the results of this analysis as well as the results for the SASSI analysis for the JOS\_L ground motion, and shows that the SASSI and LS-DYNA results are virtually identical when foundation nonlinearities are eliminated. Although the peak input acceleration at the base of the soil profile is 0.06g, the peak acceleration at the free-field is 0.15g (Figure 14), and the peak roof acceleration is 0.45g (Figure 16) indicating considerable amplification for the JOS\_L ground motion, which results in nonlinear footing response. This amplification occurs because both the soil profile and the structure have a natural period and flexible-base period, respectively, of about 0.6 sec, which also corresponds to the peak in the acceleration response spectrum of the input at the base (Figure 9).

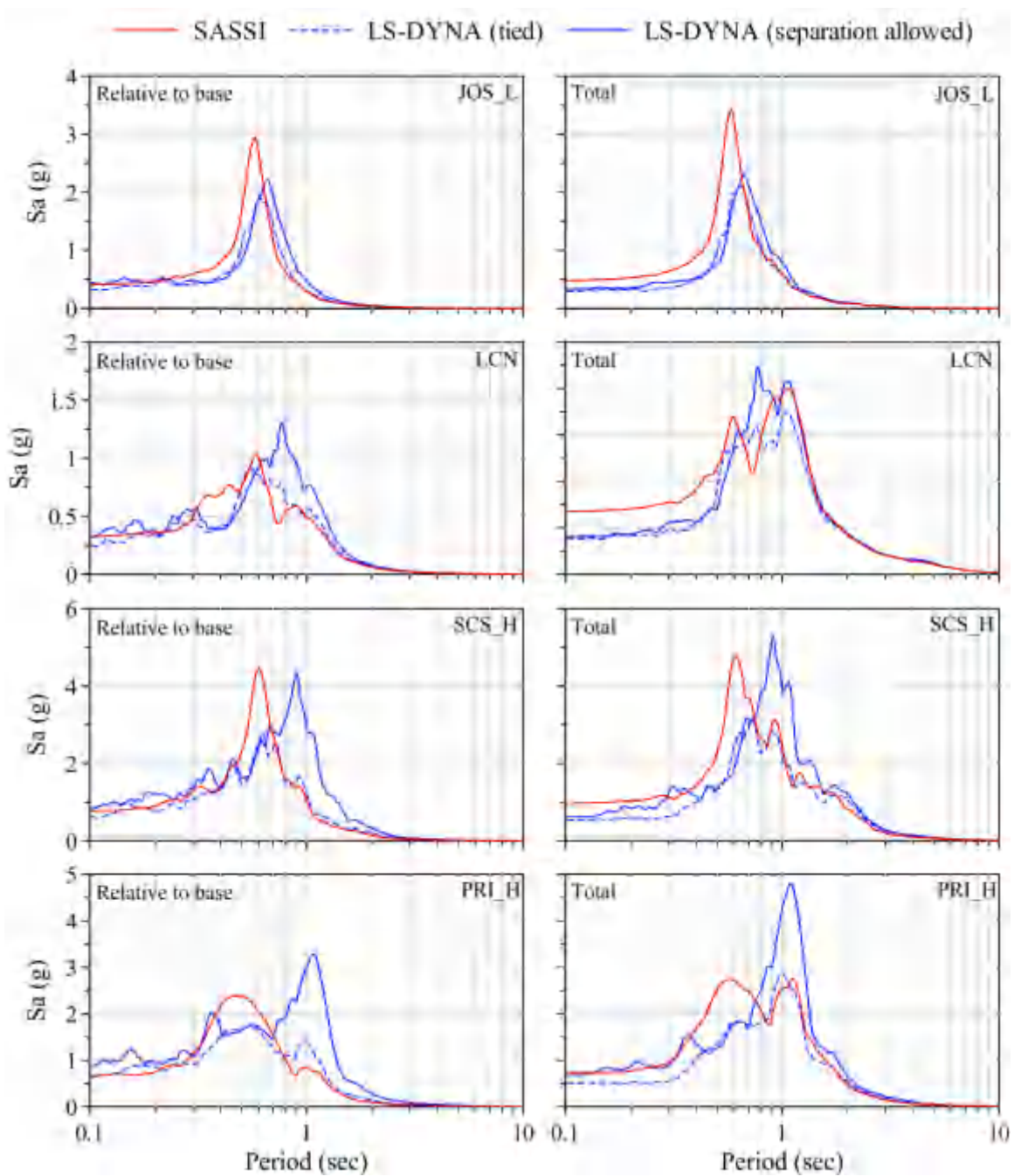


**Figure 16:** Acceleration response spectra (5% damping) at the roof of MS1F\_2 calculated using strain-compatible soil properties in SASSI, and nonlinear soil properties in LS-DYNA

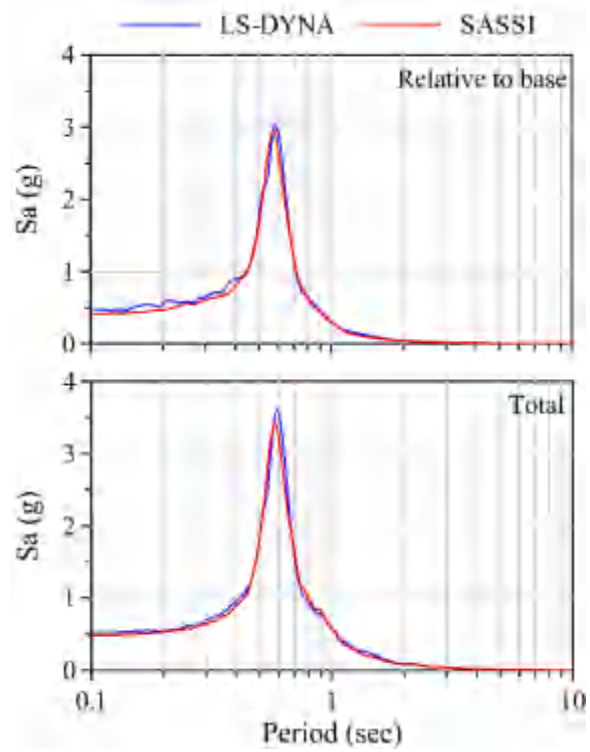


**Figure 17:** Acceleration response spectra (5% damping) at the roof of MS1F\_2 subjected to the JOS\_L ground motion calculated using strain compatible soil properties in SASSI and nonlinear soil properties in LS-DYNA but ignoring nonlinear soil behavior at the vicinity of the footings

Figure 16 also shows that preventing separation at the foundation-soil interface in the LS-DYNA model by using a tied foundation condition significantly changes the response. Specifically, the peaks of the relative acceleration spectra occur at a shorter period (which is still longer than the period corresponding to the SASSI responses), and the amplitudes of these peaks are smaller than the LS-DYNA case that allows separation at the foundation. Additionally, the differences between the LS-DYNA results for the tied interface and the SASSI results are also significant, indicating that the nonlinear response due to geometric nonlinearities (gapping, sliding and uplift) and soil hysteresis are both considerable. Whereas nonlinear soil hysteresis results in an elongation of the period of peak spectral acceleration (not captured in the SASSI analysis), the loss of contact due to gapping and uplift reduces the hysteretic damping, and consequently results in an increase in the peak spectral acceleration by comparison with the tied foundation case. In summary, the results presented in Figure 16 show the significant impact of geometric nonlinearities, including sliding and gapping of the footings as well as the hysteretic

behavior of soil at the footing vicinity, on the MS1F\_2 response. Geometric nonlinearities, in particular, result in greater peak spectral accelerations that occur at longer periods compared with the equivalent-linear response, which is contrary to the widely held assumption that nonlinear behavior at foundation results in a reduction in the spectral response.

Yielding of the beams in the fuses is observed in the LS-DYNA response to the PRI\_H ground motion when separation at the foundation-soil interface is allowed. However, no yielding is observed in the corresponding LS-DYNA response for the tied foundation case, indicating that gapping and sliding of the footings resulted in increased ductility demands in the beams. No yielding is observed in the beams for the other ground motions for both the LS-DYNA cases. SASSI cannot directly capture yielding in a superstructure.

#### 4.5.3 MS1F\_2 retrofitted with grade beams

Grade beams that connect the footings are used in practice to prevent the differential horizontal displacement of footings. Grade beams can also restrain the independent rocking of footings. The change in structural behavior by restraining footings using grade beams is investigated here because of the observed significance of relative horizontal footing displacement on the response of MS1F\_2. Rigid grade beams are simulated in LS-DYNA by constraining all the rigid footings to move together, acting as a single rigid body. Rigid grade beams in SASSI are explicitly modeled as very stiff beams connecting the bases of the columns.

Figure 18 presents the SASSI and LS-DYNA responses of MS1F\_2 equipped with rigid grade beams. The LS-DYNA response accounts for separation at the foundation-soil interface. The results presented in this figure are markedly different from the responses of MS1F\_2 without grade beams. Firstly, the responses calculated from SASSI and LS-DYNA for the modified structure with grade beams are much closer than those calculated for the original structure (Figure 16). This observation holds for relative accelerations as well as the total accelerations at the roof, and indicates that using grade beams reduces secondary nonlinearities at the vicinity of the footings. Secondly, although the period of maximum spectral acceleration (relative to the base) remains almost unchanged for the SASSI responses, it decreases significantly for the LS-DYNA responses (in comparison with the case without grade beams). Thirdly, the peak spectral accelerations of modified MS1F\_2 are slightly smaller than those calculated for the original structure for all but the JOS\_L ground motion. These differences are all primarily due to the

reduced gapping and sliding of the footings when grade beams are constructed, which reduces nonlinear behavior in the soil near the footings. Figure 18 also shows a significant reduction in the peak spectral acceleration at the roof of the modified structure for the PRI\_H ground motion. The SSI period of the original structure (about 1.2 sec) coincides with the spectral peak in the free-field response for this ground motion. Using grade beams reduces the SSI period to about 0.45 sec, and therefore reduces the peak spectral acceleration at the roof of the modified structure.

No yielding is observed in the beams of MS1F\_2 equipped with grade beams, even for the PRI\_H ground motion. The grade beams prevent differential horizontal movement of the footings: footing spreading. The footings in the original structure slide and rock independently, resulting in footing spreading, which increases the bending moment in the beams at the roof level. Grade beams restrict the footing spreading and result in smaller moment demands in the beams. Figure 19 presents the displacement histories of two adjacent footings along the X-direction for both the original and modified MS1F\_2 subjected to the PRI\_H ground motion. Footings 1 and 2 in the figure correspond to the left-hand side and right-hand side footings of the structure, when facing in the positive Y-direction. Footing 2 shows larger residual displacements than footing 1 for the original structure, indicating relative lateral displacement. The footings of modified MS1F\_2 have identical displacements. Figure 19 also presents screenshots of the deformed LS-DYNA models of the original and modified structures. The figure clearly shows the reduction in footing displacements when grade beams are used.

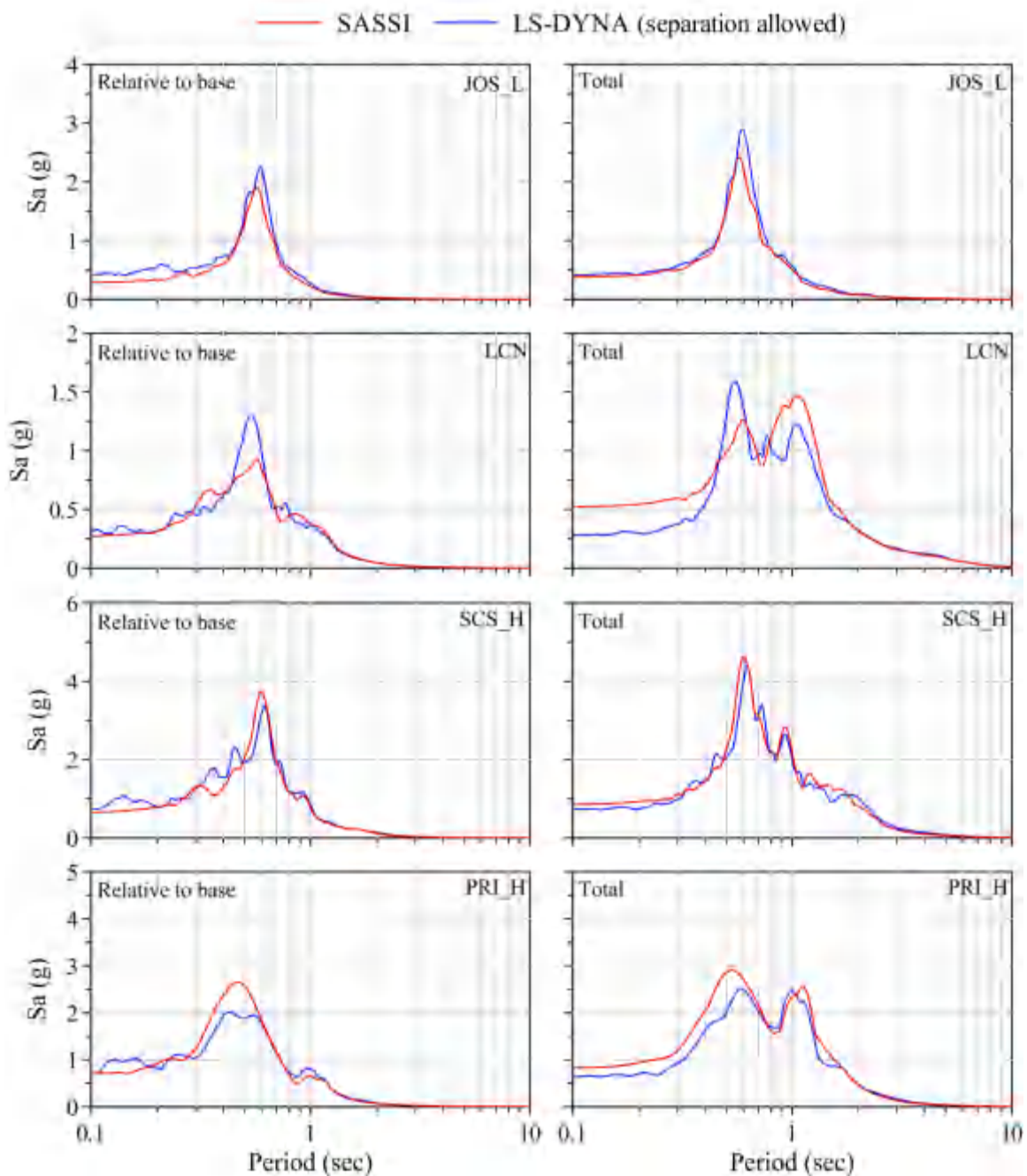


**Figure 18:** Relative and total acceleration response spectra (5% damping) at the roof of MS1F\_2 equipped with grade beams, calculated using strain-compatible soil properties in SASSI, and nonlinear soil properties in LS-DYNA

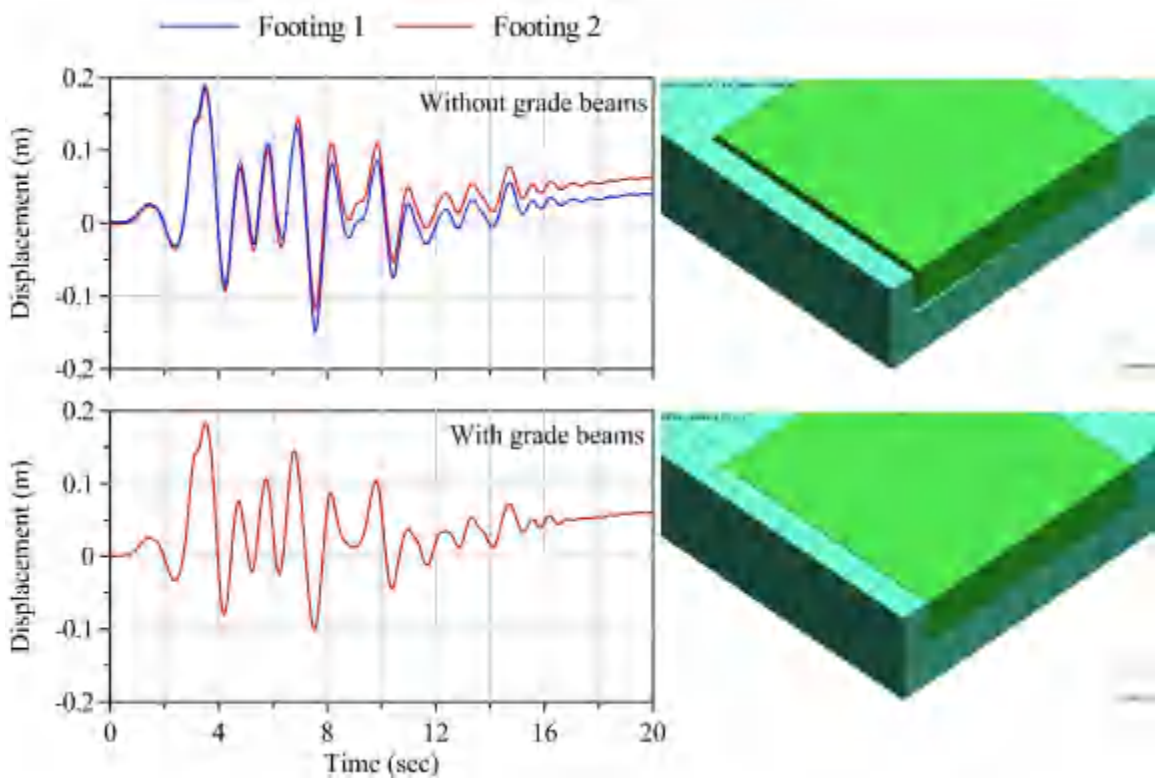


**Figure 19:** Time series of the horizontal displacement and the corresponding screenshots of two adjacent footings of MS1F\_2 (along the X direction) for the PRI\_H ground motion

#### 4.5.4 MS2F

Similar to MS1F\_2, a linear elastic analysis is first performed for MS2F subjected to the JOS\_L ground motions using strain-compatible moduli and 2% damping ratio for the soil in both SASSI and LS-DYNA. Results for this analysis are presented in Figure 20. The figure shows that the SASSI and LS-DYNA responses are very similar, confirming that the corresponding numerical models are equivalent in the linear domain.

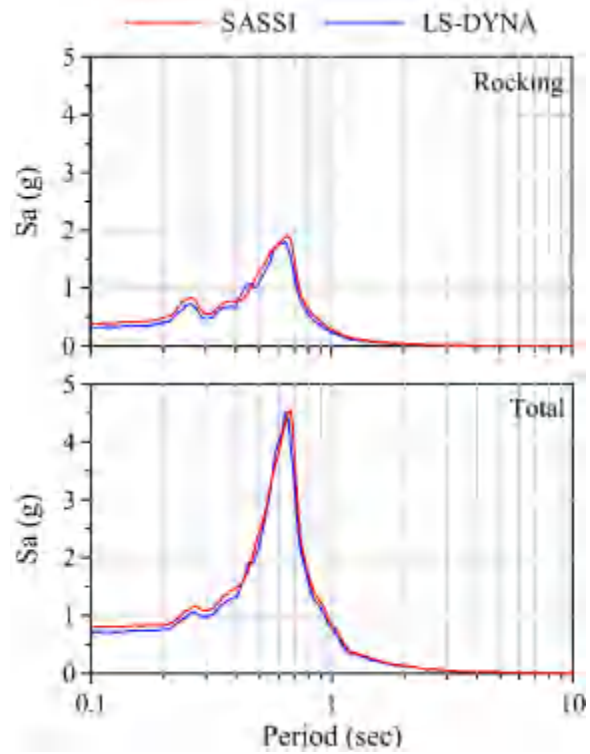


**Figure 20:** Acceleration response spectra (5% damping) at the roof of MS2F subjected to the JOS\_L ground motion calculated using strain-compatible moduli and 2% damping ratio for the soil

Following the verification of the numerical models for linear analysis, nonlinear analyses in LS-DYNA and equivalent-linear analyses in SASSI are performed for the four ground motions introduced previously. Similar to MS1F\_2, two contact models ('tied' and 'separation-allowing') are employed for the foundation-soil interface. Figure 21 presents the 5% damped response spectra of the roof accelerations (rocking accelerations in the left panels and total accelerations in the right panels) calculated using SASSI and LS-DYNA. The figure shows that the SASSI and LS-DYNA responses (for both cases) are closer than those calculated for MS1F\_2 without grade beams, indicating that the foundation nonlinearities in MS2F are smaller than those observed in MS1F\_2. This is expected since MS2F is founded on a basemat, while MS1F\_2 is founded on spread footings. Figure 21 also shows that there is a small increase in the peak spectral accelerations calculated using LS-DYNA, when separation is enabled at the foundation-soil interface. This increase is attributed to a reduction in the hysteretic damping in the foundation from the tied-foundation case, as a result of the loss of contact during rocking and sliding.

Although sliding should result in additional energy dissipation, it does not result in a net reduction in the spectral accelerations because MS2F responds predominantly in rocking. This observation supports a prior statement that geometric nonlinearities may result in an increase in peak spectral acceleration, depending on the relative degree of sliding (an energy dissipating mechanism), gapping and uplift (that reduce energy dissipation).

Figure 21 also shows that although the SASSI and LS-DYNA responses are similar for the JOS\_L ground motion, the peak spectral responses of the total acceleration are smaller than those calculated using SASSI for the other three ground motions. (Bolisetti and Whittaker (2015) present a comparison of the responses calculated using linear and nonlinear methods, and that information is not repeated here.) This is primarily because of the underestimation of the free-field response by LS-DYNA as compared with SASSI [a typical trend in the differences between linear and nonlinear site responses; see Bolisetti *et al.* (2014)].

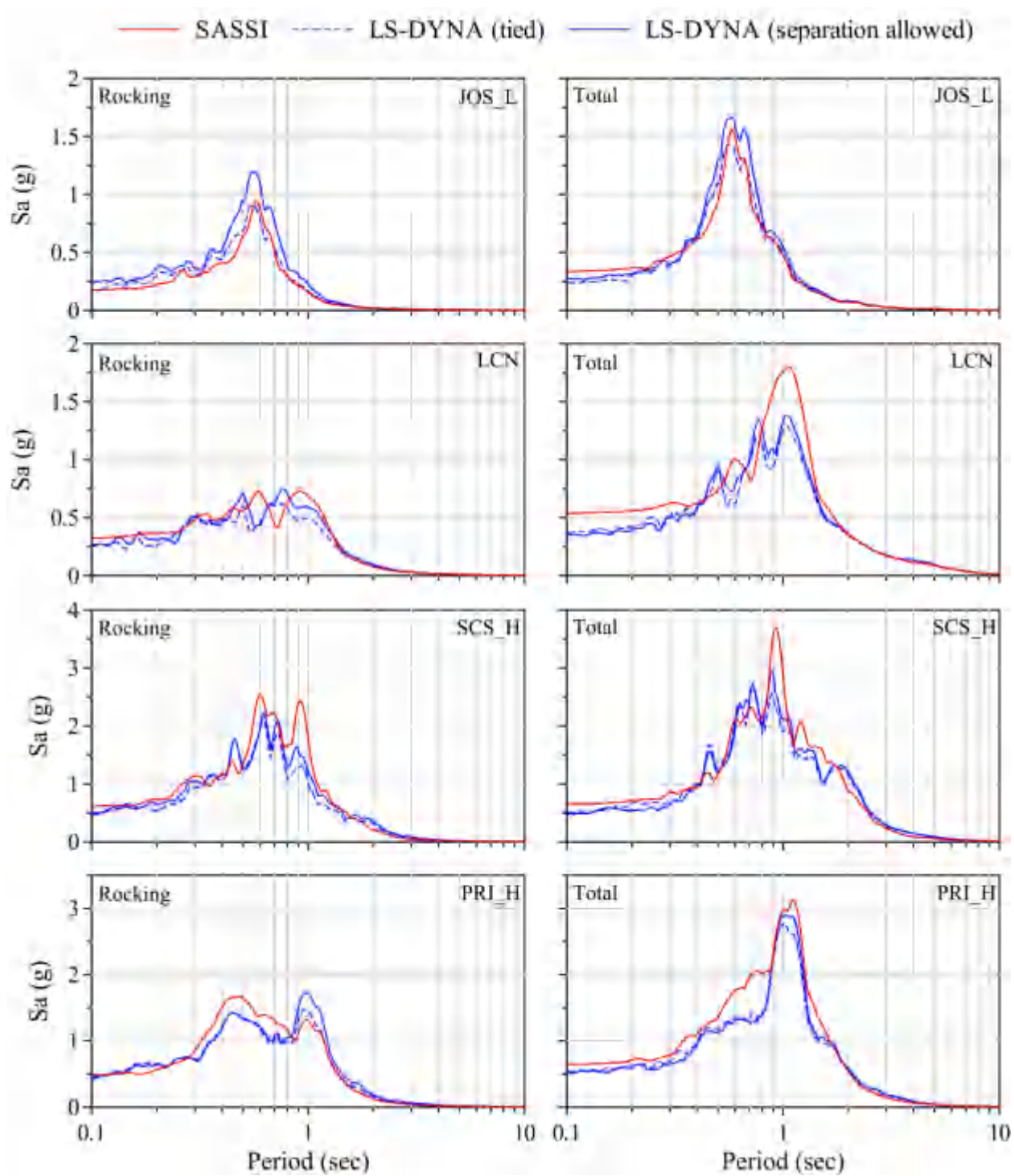


**Figure 21:** 5% damped acceleration response spectra at the roof of MS2F calculated using strain-compatible soil properties in SASSI, and nonlinear soil properties in LS-DYNA

## **5. Summary and conclusions**

This paper presents an assessment of the industry-standard SSI analysis codes, SASSI and LS-DYNA for linear and nonlinear SSI analyses of safety-related nuclear structures and commercial buildings. The first step in the assessment is to benchmark the time-domain code LS-DYNA against the frequency-domain code SASSI, for linear SSI analyses. This is accomplished by performing linear SSI analyses of two idealized, lumped mass structures using SASSI and LS-DYNA, and verifying that the analysis procedures employed in the two codes provide almost identical responses. The second part of the assessment extends these analysis procedures to structures and soil profiles that exhibit nonlinear behavior. The nonlinear SSI responses are calculated for a one-story steel-moment resisting frame building founded on spread footings and a two-story shear-wall building founded on a basemat, subjected to four recorded input ground motions of different intensities. The responses are calculated in SASSI using strain-compatible moduli and damping ratios for the soils. LS-DYNA analyses are performed using two soil-foundation interfaces: 1) an interface that is tied and does not allow separation (gapping and sliding) between the soil and the foundation, and 2) an interface that allows separation between the soil and the foundation. The responses calculated using SASSI and LS-DYNA are compared for all the ground motions.

The following conclusions can be drawn from the studies presented in this paper:

1. The frequency-domain code, SASSI and the time-domain code, LS-DYNA, result in almost identical responses for SSI analyses of linear models. This is an important result in the benchmarking of time-domain codes against the frequency-domain codes for linear analyses.
2. Nonlinear SSI predictions can be significantly different from those made using linear frequency-domain codes. The differences are greatest for cases with significant nonlinearities, such as nonlinear site response (primary nonlinearities) and nonlinear behavior at the foundation (secondary nonlinearities), namely, soil hysteresis, and gapping and sliding underneath the foundation. In the study presented in this paper, the responses of a one-story structure on surface-mounted, independent spread footings, calculated using SASSI and LS-DYNA, differed considerably due to nonlinear response at the soil-foundation interface as well as in the soil around the footings.

3. Nonlinear response at the vicinity of the foundations (secondary nonlinearities) can be significant in near-surface founded buildings. Geometric nonlinearities, in particular, can lead to an increase in superstructure demands depending on the relative degree of sliding (an energy dissipating mechanism) and gapping and uplift (that reduce energy dissipation). A considerable increase in the roof accelerations of the one-story structure is observed when modeled with a soil-footing interface that simulates separation, as opposed to an interface that does not allow separation between the soil and the footing. Ignoring geometric nonlinearities may therefore result in an unconservative prediction of the superstructure response. In the context of performance-based design, nonlinear SSI effects should therefore be considered in buildings if accurate estimates of loss are required.
4. Structures with independent spread footings are susceptible to increased component ductility demands due to relative horizontal footing displacement. Connecting footings with grade beams will eliminate this relative displacement and potentially reduce ductility demands in the superstructure.

Nonlinear material models of soils and contact models have not yet been formally validated using either experimental or field data. Validation of such models is an important step towards the greater use of nonlinear SSI analysis. Studies are underway in a 1D geotechnical laminar box at the University at Buffalo to assemble laboratory data suitable for validating numerical models.

The results of this study are also significant for the SSI analysis of safety-related nuclear structures and buildings subjected to beyond-design basis earthquake shaking. Although the structural and soil characteristics encountered at the sites of nuclear facilities are generally different from those adopted for this study, the results presented here show that soil and structural responses calculated using frequency-domain codes can deviate significantly from the theoretically more accurate time-domain codes for those analysis cases involving significant nonlinear behavior.

## Acknowledgments

This study was funded by the US National Science Foundation (NSF) under Grant No. CMMI-0830331, MCEER at the University at Buffalo, State University of New York, and the United States Department of Energy. The authors acknowledge this financial support. The opinions, findings, conclusions and recommendations expressed in this paper are those of the

authors alone. The authors thank Ibrahim Almufti and Michael Willford at Arup, San Francisco for providing valuable guidance in performing SSI analysis in LS-DYNA.

## **References:**

- Anderson, L. M., Elkhoraibi, T., and Ostdan, F. (2013). "Validation of SASSI2010 Solution Methods through Independent Verification Using SAP2000 for Deeply Embedded Structures with Large Footprints." 22nd International Conference in Structural Mechanics in Reactor Technology - SMiRT 22, August 2013, San Francisco, California.
- ANSYS Inc. (2013). Computer Program ANSYS 13.0, ANSYS Inc., Canonsburg, Pennsylvania.
- Basu, U. (2009). "Explicit Finite Element Perfectly Matched Layer for Transient Three-Dimensional Elastic Waves." International Journal for Numerical Methods in Engineering, 77, 151-176.
- Basu, U. (2011). "Soil-Structure Interaction." <[http://www.lstc.com/applications/soil\\_structure](http://www.lstc.com/applications/soil_structure)>.
- Bielak, J. (1975). "Dynamic Behaviour of Structures with Embedded Foundations." Earthquake Engineering & Structural Dynamics, 3, 259-274.
- Bielak, J., and Christiano, P. (1984). "On the Effective Seismic Input for Nonlinear Soil-Structure Interaction Systems." Earthquake Engineering & Structural Dynamics, 12(1), 107-119.
- Bielak, J., Loukakis, K., Hisada, Y., and Yoshimura, C. (2003). "Domain Reduction Method for Three-Dimensional Earthquake Modeling in Localized Regions, Part-I: Theory." Bulletin of the Seismological Society of America, 93(2), 817-824.
- Bolisetti, C., and Whittaker, A. S. (2015). "Site Response, Soil-Structure Interaction and Structure-Soil-Structure Interaction for Performance Assessment of Buildings and Nuclear Structures." Report MCEER 15-0002, University at Buffalo, The State University of New York, Buffalo, NY.
- Bolisetti, C., Whittaker, A. S., Mason, H. B., Almufti, I., and Willford, M. (2014). "Equivalent Linear and Nonlinear Site Response Analysis for Design and Risk Assessment of Safety-Related Nuclear Structures." Nuclear Engineering and Design, 275, 107-121.

Chiang, D. Y. and Beck, J. L. (1994). "A New Class of Distributed-Element Models for Cyclic Plasticity - I. Theory and Application." International Journal of Solids and Structures, 31(4), 469-484.

Coleman, J. L., Bolisetti, C., Whittaker, A. S. (2015). "Time-Domain Soil-Structure Interaction Analysis for Nuclear Facilities." Nuclear Engineering and Design, 298, 264-270.

Computers and Structures Inc. (2011). Computer Program SAP2000 - Structural Analysis Program, Version 11.0.0, Computers and Structures, Inc., Berkeley, California.

Coronado, C., Anderson, L. M., and Ostadan, F. (2013). "Verification of SASSI Extended Subtraction Method for Computing the Seismic Response of Deeply Embedded Structures." 22nd International Conference in Structural Mechanics in Reactor Technology - SMiRT 22, August 2013, San Francisco, California.

Dassault Systèmes (2005). Computer Program ABAQUS - Finite Element Analysis Software, Dassault Systèmes, Providence, Rhode Island.

Day, S. M., Bielak, J., Dreger, D., Graves, R., Larsen, S., Olsen, K. B., Pitarka, A., and Guzman, L. R. (2006). "Numerical Simulation of Basin Effects on Long Period Ground Motion." Proceedings: Proceedings of the 8th U.S. National Conference on Earthquake Engineering, San Francisco, California.

Gaston, D., Newman, C., Hansen, G., and Lebrun-Grandi'e, D. (2009). "MOOSE: A Parallel Computational Framework for Coupled Systems of Nonlinear Equations." Nuclear Engineering and Design, 239, 1768-1778.

Iwan, W. (1967). "On a Class of Models for the Yielding Behavior of Continuous and Composite Systems." Journal of Applied Mechanics, 34(E3), 612–617.

Jeremić, B., Jie, G., Preisig, M., and Tafazzoli, N. (2009). "Time Domain Simulation of Soil-Foundation-Structure Interaction in Non-Uniform Soils." Earthquake Engineering & Structural Dynamics, 38(5), 699-718.

Kramer, S. L. (1996). "Geotechnical Earthquake Engineering." Prentice Hall, Upper Saddle River, New Jersey.

Kulhawy, F. H., and Mayne, P. W. (1990). "Manual on Estimating the Soil Properties for Foundation Design." Report EL-6800, Electric Power Research Institute, Palo Alto, California.

Livermore Software Technology Corporation (LSTC). (2013). "LS-DYNA Keyword User's Manual - Version R 7.0." Livermore Software Technology Corporation, Livermore, California.

Lysmer, J., and Kuhlemeyer, R. L. (1969). "Finite Dynamic Model for Infinite Media." Journal of Engineering Mechanics Division, 95, EM4, 859-877.

Lysmer, J., Ostadan, F., and Chin, C. (1999). Computer Program SASSI2000 - A System for Analysis of Soil-Structure Interaction, University of California, Berkeley, California.

Mason, H. B., Kutter, B. L., Bray, J. D., Wilson, D. W., and Choy, B. Y. (2010). "Earthquake Motion Selection and Calibration for Use in a Geotechnical Centrifuge." Proceedings: 7th International Conference on Physical Modelling in Geotechnics, Campus Science City (Hönggerberg), ETH, Zurich, Switzerland.

Mason, H. B. (2011). "Seismic Performance Assessment in Dense Urban Environments." Ph.D. Dissertation, University of California, Berkeley, California.

Mason, H. B., Trombetta, N. W., Gille, S., Lund, J., Zupan, J., Jones, K. C., Puangnak, H., Bolisetti, C., Bray, J., Hutchinson, T., Fiegel, G., Kutter, B. L., and Whittaker, A. S. (2010a). "Seismic Performance Assessment in Dense Urban Environments: Centrifuge Data Report for HBM02 (Test 1)." University of California at Davis Center for Geotechnical Modeling, Davis, California.

Mason, H. B., Trombetta, N. W., Gille, S., Lund, J., Zupan, J., Jones, K. C., Puangnak, H., Bolisetti, C., Bray, J., Hutchinson, T., Fiegel, G., Kutter, B. L., and Whittaker, A. S. (2010b). "Seismic Performance Assessment in Dense Urban Environments: Centrifuge Data Report for HBM03 (Test 2)." University of California at Davis Center for Geotechnical Modeling, Davis, California.

Mason, H. B., Trombetta, N. W., Gille, S., Lund, J., Zupan, J., Jones, K. C., Puangnak, H., Bolisetti, C., Bray, J., Hutchinson, T., Fiegel, G., Kutter, B. L., and Whittaker, A. S. (2011). "Seismic Performance Assessment in Dense Urban Environments: Centrifuge Data Report for HBM04 (Test 3)." University of California at Davis Center for Geotechnical Modeling, Davis, California.

Mason, H. B. (2014). Personal Communication

Mazzoni, S., McKenna, F., Scott, M. H., and Fenves, G. L. (2009). Computer Program OpenSees: Open System for Earthquake Engineering Simulation, Pacific Earthquake Engineering Research Center (PEER), University of California, Berkeley, California.

Ostadan, F. (2006a). "SASSI2000: A System for Analysis of Soil Structure Interaction - User's Manual." University of California, Berkeley, California.

Ostadian, F. (2006b). "SASSI2000: A System for Analysis of Soil Structure Interaction - Theoretical Manual." University of California, Berkeley, California.

Ostadian, F. (2010). Personal Communication

Ostadian, F., and Deng, N. (2011). Computer Program SASSI2010 - A System for Analysis of Soil-Structure Interaction, Version 1.1, Geotechnical and Hydraulic Engineering Services, Bechtel National Inc., San Francisco, California.

Ryan, H. (1994). "Ricker, Ormsby, Klander, Butterworth - A Choice of Wavelets." Canadian Society of Exploration Geophysicists Recorder, 19(7), 8-9.

Schnabel, P. B., Lysmer, J., and Seed, H. B. (2012). Computer Program SHAKE: A Computer Program for Earthquake Response Analysis of Horizontally Layered Sites, University of California, Berkeley, California.

Seed, H. B., and Idriss, M. (1970). "Soil Moduli and Damping Factors for Dynamic Response Analysis." Report UCB/EERC 70/10, Earthquake Engineering Research Center, University of California, Berkeley, California.

Somerville, P. G., Smith, R. W., Graves, R. W., and Abrahamson, N. A. (1997). "Modification of Empirical Strong Ground Motion Attenuation Relations to Include the Amplitude and Duration Effects of Rupture Directivity." Seismological Research Letters, 68, 199-222.

Spears, R., and Coleman, J. (2014). "Nonlinear Time Domain Soil-Structure Interaction Methodology Development." INL/EXT-14-33126, Idaho National Laboratory, Idaho Falls, Idaho.

Taborda, R. (2010). "Three Dimensional Nonlinear Soil and Site-City Effects in Urban Regions." Ph.D. Dissertation, Carnegie Mellon University, Pittsburgh, Pennsylvania.

Taborda, R., and Bielak, J. (2011). "Large-Scale Earthquake Simulation: Computational Seismology and Complex Engineering Systems." Computing in Science and Engineering, 13(4), 14-27.

Trombetta, N. W. (2013). "Seismic Soil-Foundation Structure Interaction in Urban Environments." Ph.D. Dissertation, University of California, San Diego, California.

Willford, M., Sturt, R., Huang, Y., Almufti, I., and Duan, X. (2010). "Recent Advances in Nonlinear Soil-Structure Interaction Analysis using LS-DYNA." Proceedings of the NEA-SSI Workshop, October 6-8, Ottawa, Canada.

Xu, J. (1998). "Three-Dimensional Simulation of Wave Propagation in Inelastic Media on Parallel Computers with Application to Seismic Response." Ph.D. Dissertation, Carnegie Mellon University, Pittsburgh, Pennsylvania.

Xu, J., Bielak, J., Ghattas, O., and Wang, J. (2003). "Three-Dimensional Nonlinear Seismic Ground Motion Modeling in Basins." Physics of the Earth and Planetary Interiors, 137, 81-95.

Xu, J., Miller, C., Costantino, C., and Hofmayer, C. (2006). "Assessment of Seismic Analysis Methodologies for Deeply Embedded Nuclear Power Plant Structures." U.S. Nuclear Regulatory Commission, Washington, District of Columbia

Yoshimura, C., Bielak, J., and Hisada, Y. (2003). "Domain Reduction Method for Three-Dimensional Earthquake Modeling in Localized Regions, Part-II: Verification and Examples." Bulletin of the Seismological Society of America, 93(2), 825-840.

## Highlights:

- Described a method of performing time-domain nonlinear SSI analysis.
- Benchmarked this method against the established frequency-domain code, SASSI.
- Performed fully nonlinear SSI analyses of two buildings using LS-DYNA.
- Compared LS-DYNA results to those calculated using SASSI.
- Observed significant differences for cases with highly nonlinear behavior.

## Keywords

Soil-Structure Interaction; Nonlinear Soil-Structure Interaction Analysis; Earthquake Engineering; Finite-Element Analysis